Determination of the Link Lengths for a Spatial 3-DOF Parallel Manipulator

Xin-Jun Liu
e-mail: xinjunliu@mail.tsinghua.edu.cn

Jinsong Wang

Manufacturing Engineering Institute,
Department of Precision Instruments,
Tsinghua University,
Beijing, 100084,
People's Republic of China

Jongwon Kim
School of Mechanical and Aerospace Engineering,
Seoul National University,
Seoul, 151-744,
Korea

This paper addresses the issue of determining the optimal geometric parameters of a 3-DOF parallel manipulator. One of the advantages of the manipulator is that the moving platform exhibits high tilting capabilities, e.g., as much as ±50 deg. *The first step of the new optimal methodology proposed in this paper to achieve the optimum design involves developing a design space that includes all possible basic similarity manipulators. The next step deals with the graphical representation of atlases that can illustrate relationships between performance criteria and design parameters. With such atlases, the designer can identify an optimum region with respect to the specification on performances. The region contains the optimum candidates, from which we can select one directly. Finally, the geometric parameters of the manipulator can be reached by comparing the desired workspace and the good-conditioning workspace. The design methodology discussed in this paper has no process to establish the objective function and does not involve any optimization algorithm, which is normally used in traditional optimization. We expect that since each manipulator in the developed design space represents all of its similarity manipulators in terms of performances, this method will guarantee an optimum design result.* [DOI: 10.1115/1.2159028]

Keywords: parallel manipulators, optimum design, rotational capability, workspace, kinematics, design space

1 Introduction

In the past two decades, parallel manipulators have received great attention due to their properties of increased accuracy, high stiffness, high speed, compactness, and high payload capability. There are two primary important issues in the field of parallel manipulator: one is mechanical architecture design and the other is optimum design of the manipulator.

In this field, an interesting thing is finding a method to design a mechanical architecture for a parallel manipulator being given its number and type of degree of freedom (DOF). After Gough established the basic principle of a manipulator with a closed-loop kinematic structure in 1947, many other parallel manipulators with specified number and type of DOF have been proposed. It is not difficult to find that most efforts are contributed to 6-DOF parallel manipulators. However, they suffer the problems of complex forward kinematics, relatively small useful workspace, and complicated multi-DOF joints. To overcome these shortcomings, parallel manipulators with less than six DOFs, especially, that with 3 DOFs have been recently investigated. For example, Liu et al. [1] proposed a 3-DOF parallel manipulator, **HALF**, with high rotational capability thanks to all single-DOF joints that are involved in the rotational DOF. Parallel manipulators with three pure orientational DOFs were presented by Kong and Gosselin [2], Di Gregorio [3], and Hess-Coelho [4]. Kim and Tsai [5] designed a Cartesian parallel manipulator that employs only revolute and prismatic joints. Other parallel manipulators with three translations were studied by Chablat and Wenger [6], Liu et al. [7], Carricato and Parenti-Castelli [8], and Jin and Yang [9], respectively. Some new 3-DOF parallel manipulators were introduced by Liu and Wang [10].

In this paper, a modified version of **HALF** will be presented. This manipulator is intended to have a high rotational capability of as much as 100 deg in the workspace. In this paper, we will only focus on the optimum design issue of the parallel manipulator.

Design optimization of parallel manipulators is an important and challenging problem. There are two issues considered in the optimal design of the manipulator: performance evaluation and dimensional synthesis. Having designed a manipulator, it is necessary to evaluate its main characteristics. A second problem is to determine the dimensions (link lengths) of the manipulator that are suitable for the task at hand. Among these two, the latter one is one of the most difficult issues in this field. In the optimum design process, several performance criteria, such as workspace [11–16], singularity [14,17], dexterity [16,18,19], accuracy [20], stiffness [5,16,21], and conditioning index [14,22,23] can be considered to achieve design objectives. In the case of dexterity and conditioning index, the condition number of Jacobian matrix is conventionally used.

In the process of optimum design, it is of the most importance which kind of design methodology is chosen. As mentioned in [24], as some performance criteria are antagonistic and the designer may not be fully aware of all the requirements, a good design methodology should allow the designer to determine not one single solution but a set of possible solutions, and ideally, all the design solutions. The mostly commonly used methods involve, first of all, establishing the objective functions with specified constraints and then searching the result utilizing an optimization algorithm. For example, considering both the parasitic motions and the condition number, the optimization result of a 3-PRS parallel mechanism was reached by virtue of the quasi-Newton optimization algorithm [19]. In both Refs. [5,11], the sequential quadric programming was used as the solution technique for the constrained optimization problem, where in Ref. [5], the authors defined an objective function of maximizing the stiffness subjecting to a specified workspace and in [11], the objective functions were based on the manipulator size and a specified orientation workspace. In [20], the authors developed an accuracy criterion, i.e., the error amplification factor (EAF). Based on the

Contributed by the Mechanisms and Robotics Committee of ASME for publication in the JOURNAL OF MECHANICAL DESIGN. Manuscript received April 6, 2005; final manuscript received July 8, 2005. Review conducted by Madhu Raghavan

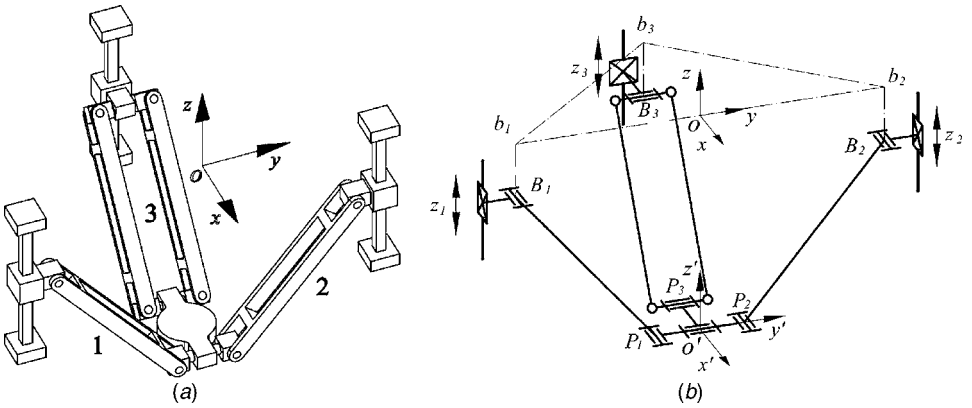

Fig. 1 New spatial 3-DOF parallel manipulator and its kinematical scheme

concept of minimizing the global EAF subjecting to singularity constraints and design variables limits, the sequential quadric programming in MATLAB was applied to obtaining the result. These methodologies have common disadvantages, i.e., the process is iterative and time consuming, and the algorithms do not ensure convergence to a global minimum for objectives with multiple minima. Recently, some algorithms, e.g., the genetic algorithm [25] and an algorithm based on interval analysis [26], which were applied to the design of parallel manipulators, were proposed. Even though these algorithms can provide a global minimum, each of the developed design methodologies can only be applied to a specified objective. If the designer decides to change the objective, s/he must start the optimization from the very beginning. In addition, these methodologies fail to visually and globally show the relationship between the objective and design parameters visually and globally. For such reasons, none of the methodologies can be a universal one or be easily incorporated with others.

To solve the abovementioned problems, here we attempt to develop a new optimum design method which can be applied to the design of a 3-DOF parallel manipulator as that no angle parameter is involved. The methodology is to first establish a design space including all involved design parameters and, second, to plot performance atlases in the space, which can clearly show the relationships between the performance criteria and design parameters. Based on these atlases, the designer can reach an optimum region with respect to specified objectives. In addition, this region provides constraint information about the design parameters and so, one can pick up a suitable group of design parameters from this region directly. The link lengths for the geometric parameters can be finally achieved by comparing the desired workspace and the *good-conditioning workspace*. One of the advantages of the methodology is that it guarantees a global optimization.

2 Spatial 3-DOF Parallel Manipulator

2.1 Description of the Manipulator. In [1], a spatial 3-DOF parallel manipulator, called the **HALF** manipulator, was proposed. The manipulator consists of a base plate, a movable platform, and three legs that connect the aforementioned two plates with each other. The detailed description about the manipulator can be found in [1]. As described in the paper, in the first and second legs, the axes for the revolute joints in the U (universal) joints that are connected to the moving platform should be collinear. And the axis of the revolute joint in the third leg linked to the moving platform should be parallel to the two axes. As two revolute joints in the first and second legs connected to the moving platform should have the same axis, they can be simplified to one revolute joint, i.e., the two U joints can be replaced by three revolute joints. The kinematic chain of the new manipulator is $^{PRR}_{PRR}$R−PR(Pa)R, where (Pa) stands for planar four-bar parallelogram, P prismatic joint and R revolute joint. Figure 1 shows the modified parallel manipulator and its kinematical scheme.

The modified manipulator has exactly the same capability as the **HALF** manipulator, i.e., two translational DOFs in the *O-yz* plane and one rotational DOF about the *y* axis. One of the distinct advantages of the parallel manipulator is that the rotational DOF has high orientational capability.

The modified manipulator studied here exhibits a morphology identical to **HALF** manipulator. This means that the inverse kinematic problem, Jacobian matrix and singularity of the modified manipulator can be solved using the same methods described in [1]. For convenience, let us recall these problems briefly.

2.2 Inverse Kinematic Problem. A kinematical scheme of the manipulator is developed as shown in Fig. 1(*b*), where the notation is the same as that used in the **HALF** manipulator. Therefore, for a given manipulator and for prescribed values of the position (y,z) and orientation ϕ of the moving platform, the required actuator inputs can be obtained as

$$z_1 = \pm\sqrt{R_2^2-(R_3-R_1+y)^2}+z \tag{1}$$

$$z_2 = \pm\sqrt{R_2^2-(R_1+y-R_3)^2}+z \tag{2}$$

$$z_3 = \pm\sqrt{R_2^2-(R_3-R_1\cos\phi)^2-y^2}+R_1\sin\phi+z \tag{3}$$

where $R_1=O'P_i$, $R_2=P_iB_i$ and $R_3=Ob_i$ $(i=1,2,3)$. From Eqs. (1)–(3), we can see that there are eight inverse kinematic solutions for a given pose of the parallel manipulator. That means the manipulator has eight assembly modes. The assembly mode shown in Fig. 1 corresponds to the solution that each one of the signs "±" in Eqs. (1)–(3) is "+." This is exactly what we are concerned with in this paper.

2.3 Jacobian Matrix. The velocity equation can be written as

$$\mathbf{A}\dot{\boldsymbol{\rho}}=\mathbf{B}\dot{\mathbf{p}} \text{ or } \dot{\boldsymbol{\rho}}=\mathbf{J}\dot{\mathbf{p}} \tag{4}$$

where $\dot{\mathbf{p}}$ is the vector of output velocities defined as

$$\dot{\mathbf{p}}=(\dot{y}\ \dot{z}\ \dot{\phi})^{\mathrm{T}} \tag{5}$$

and $\dot{\boldsymbol{\rho}}$ is the vector of input velocities defined as

$$\dot{\boldsymbol{\rho}}=(\dot{z}_1\ \dot{z}_2\ \dot{z}_3)^{\mathrm{T}} \tag{6}$$

Matrices **A** and **B** can be expressed as

$$\mathbf{A}=\begin{bmatrix} z-z_1 & 0 & 0 \\ 0 & z-z_2 & 0 \\ 0 & 0 & R_1\sin\phi+z-z_3 \end{bmatrix} \tag{7}$$

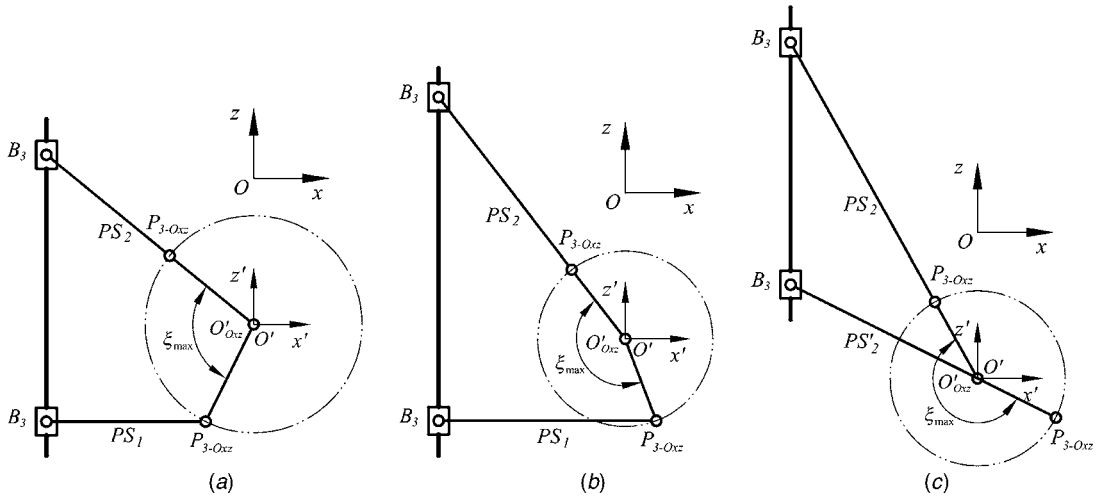

Fig. 2 Three cases of the MRC: (a) $R_2' \leq R_3$; (b) $R_3+R_1 \geq R_2' > R_3$; (c) $R_3+R_1 < R_2'$

$$\mathbf{B} = \begin{bmatrix} R_3 - R_1 + y & z - z_1 & 0 \\ R_1 + y - R_3 & z - z_2 & 0 \\ y & R_1 \sin\phi + z - z_3 & R_3 R_1 \sin\phi + R_1(z - z_3)\cos\phi \end{bmatrix} \tag{8}$$

Then, if matrix **A** is nonsingular the Jacobian matrix **J** of the manipulator can be obtained as

$$\mathbf{J} = \mathbf{A}^{-1}\mathbf{B} \tag{9}$$

2.4 Singularity. As analyzed in [1], the three kinds of singularities of the manipulator can be reached based on the analysis of matrices **A** and **B**, respectively. The first kind of singularity is the configuration whenever one of the legs P_1B_1, P_2B_2 and P_3B_3 is in the plane paralleling to the *O-xy* plane. The second kind of singular configuration occurs when the third leg P_3B_3 is in the plane defined by P_1, P_2 and P_3, or $R_1=0$. The third one is the architecture singularity. For the parallel manipulator concerned here, either $R_3=R_1+R_2$ or $R_3=R_1$ will lead to this type of singularity.

3 Characteristics of the Manipulator

In the design process, the generally used method is to determine the actuation limit with respect to the specification on the workspace and orientational capability of a manipulator, but not conversely. Then, if the actuation limit is disregarded, the manipulator described in Sec. 2 will have some unique characteristics, which are summarized below.

PROPOSITION 1. *If a parallel manipulator is actuated vertically, the Jacobian matrix is independent of the corresponding coordinate*.

Proof. For the parallel manipulator studied here, the actuation is vertically along the z axis. From the inverse kinematics of the manipulator, one can write

$$z_i - z = u_i(R_1,\ R_2,\ R_3,\ \phi,\ y), \quad i = 1,2,3 \tag{10}$$

where, $u_1=\sqrt{R_2^2-(R_3-R_1+y)^2}$, $u_2=\sqrt{R_2^2-(R_1+y-R_3)^2}$, and $u_3=\sqrt{R_2^2-(R_3-R_1\cos\phi)^2-y^2+R_1\sin\phi}$ for the assembly mode shown in Fig. 1. Substituting Eq. (10) into Eq. (9) yields

$$\mathbf{J} = \begin{bmatrix} \dfrac{R_3 - R_1 + y}{-u_1} & 1 & 0 \\ \dfrac{R_1 + y - R_3}{-u_2} & 1 & 0 \\ \dfrac{y}{R_1\sin\phi - u_3} & 1 & \dfrac{R_3 R_1 \sin\phi - R_1 u_3 \cos\phi}{R_1\sin\phi - u_3} \end{bmatrix} \tag{11}$$

from which one can see that there is no z in this matrix.

PROPOSITION 2. *The maximal rotational capability (MRC) is defined as the included angle between the singular configurations of the moving platform. The MRC of the manipulator studied here is independent of z axis*.

Proof. The MRC can be determined by the singularities of the third leg. The singularities are the configuration that the link P_3B_3 is in the plane paralleling to the *O-xy* plane and that where the link P_3B_3 is in the plane defined by P_1, P_2 and P_3, respectively. Supposing that the moving platform moves within its workspace, the projections of P_3 and O' on *O-xz* plane are denoted as P_{3-Oxz} and O'_{Oxz}, respectively. When the link P_3B_3 is in the plane paralleling to the *O-xy* plane, the configuration of the third leg is denoted as PS_1, while PS_2 and PS_2' are the corresponding configurations of the third leg when P_3B_3 and the moving platform are completely extended and folded, respectively. Then, as shown in Fig. 2, the MRC (denoted as $\xi_{\max}$) can be written as

$$\xi_{\max} = \begin{cases} \dfrac{180\ \text{deg}}{\pi}\left[\cos^{-1}\left(\dfrac{R_3}{R_1+R_2'}\right) + \cos^{-1}\left(\dfrac{R_3-R_2'}{R_1}\right)\right], & \text{if } R_2' \leq R_3 \\ \dfrac{180\ \text{deg}}{\pi}\left[\cos^{-1}\left(\dfrac{R_3}{R_1+R_2'}\right) + \dfrac{\pi}{2} + \sin^{-1}\left(\dfrac{R_2'-R_3}{R_1}\right)\right], & \text{if } R_3+R_1 \geq R_2' > R_3 \\ \dfrac{180\ \text{deg}}{\pi}\left[\cos^{-1}\left(\dfrac{R_3}{R_1+R_2'}\right) + \dfrac{\pi}{2} + \sin^{-1}\left(\dfrac{R_3}{R_2'-R_1}\right)\right], & \text{if } R_2' > R_3+R_1 \end{cases} \tag{12}$$

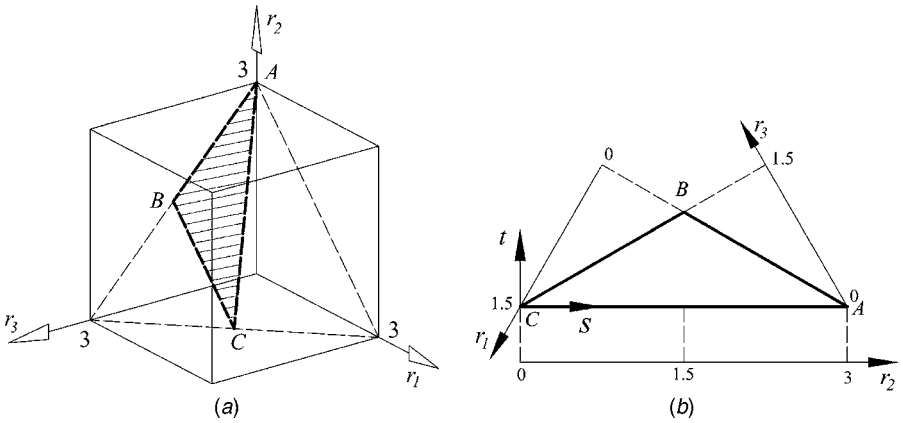

Fig. 3 Proposed design space

where $R_2'=B_3P_{3-Oxz}=\sqrt{R_2^2-y^2}$. Thus, the MRC is only related to y and the three parameters $R_i(i=1,2,3)$. Therefore, in the performance analysis we can consider only the MRC along the y axis.

Deduction 1. For the manipulator studied here, the performance indices that are defined with respect to the Jacobian matrix are also independent of z. In the performance analysis of the manipulator, the workspace along the z axis can be disregarded. Therefore, the optimum design of the manipulator can be implemented with respect to the workspace along the y axis.

PROPOSITION 3. *The distribution of the maximal rotational capability (MRC) along the y axis is symmetric about the z axis. And the MRC is maximal when* $y=0$ *and reaches its minimum at the two end points of the workspace along the y axis*.

This proposition can be proved easily. The sign (negative or positive) of y has no influence on $R_2'=\sqrt{R_2^2-y^2}$ and the MRC $\xi_{\max}$. From Fig. 2, one can see that the longer the R_2', the larger the MRC. R_2' is maximal when $y=0$ and reaches its minimum at the end points of the workspace along the y axis.

Deduction 2. If the rotational capability at one of the end points of the workspace along the y axis satisfies the specification of the manipulator, the moving platform can reach the desired tilting capability at any point within its workspace.

4 Dimension Optimization of the Parallel Manipulator

The objective of optimum design is to determine the dimension of geometric parameters of a manipulator that is suitable for the task at hand. But, before that, the desired performances should be specified. In this paper, in order to present an example of the new design method, only positional workspace and rotational capability are specified. The desired positional workspace is a region $y\times z=10$ mm $\times 10$ mm in O-yz plane without singularity. And the desired tilting capability of the moving platform is ±50 deg at every point in the workspace.

4.1 Development of a Design Space. Since the performance atlas can show the relationship between a performance and design parameter(s) visually, it is very useful in the machine design and appeared in most of design manuals. Here, we extend the design concept to our manipulator. By doing so, the most important issue in this process would be the presentation of relationship between performances and link lengths. To this end, it is of primary importance to find a tool with which it will be possible to illustrate the relationship. Then this tool can be used to obtain a performance atlas with which it will not be difficult to find the optimum result.

For the manipulator studied here, there are three geometric parameters R_1, R_2, and R_3, which are identical in their dimensions. Notice that each of three parameters can have any value between zero and infinite. This is actually the greatest difficulty, that is, to develop a design tool that can embody all manipulators (with different link lengths) within a finite space. For this reason, we must eliminate the physical link size of the manipulators. Let

$$D=(R_1+R_2+R_3)/3 \tag{13}$$

One can obtain three non-dimensional parameters r_i by means of

$$r_i=R_i/D, \quad i=1,2,3 \tag{14}$$

This would then yield

$$r_1+r_2+r_3=3 \tag{15}$$

This process makes it possible to reduce a three-dimensional problem to a two-dimensional one. Theoretically, the three non-dimensional parameters r_1, r_2, and r_3 can have any value between 0 and 3. For the parallel manipulator studied here, the three parameters should be

$$0<r_1,\ r_2,\ r_3<3,\ r_1<r_3, \quad \text{and } r_1+r_2>r_3 \tag{16}$$

in which, the inequality $0<r_1,r_2,r_3<3$ is from Eq. (15), and the two others are actually obtained from the singularity conditions in Sec. 2.4. Based on Eqs. (15) and (16), one can establish a design space as shown in Fig. 3(a), in which the triangle ABC is actually our target. In Fig. 3(a), the triangle ABC is restricted by r_1, r_2 and r_3. Therefore, it can be figured in another form as shown in Fig. 3(b), which is called the planar-closed configuration of the design space and is more convenient for us to plot an atlas.

For convenience, two orthogonal coordinates s and t are utilized to express r_1, r_2 and r_3. Thus, by using

$$\begin{cases} s=r_2 \\ t=\sqrt{3}-2r_1/\sqrt{3}-r_2/\sqrt{3} \end{cases} \tag{17}$$

coordinates r_1, r_2, and r_3 can be transformed into s and t. Equation (17) is useful for constructing a performance atlas.

4.2 Performance Evaluation and Atlas. In the design process, some performance indices will need to be included. Normally, the workspace and conditioning index (CI) are necessary criteria. In this section, the performance indices will be defined and investigated. The established design space will be used to study the relationship between the indices and link lengths, which will be presented by performance atlases. The parameters of a manipulator in this space are nondimensional. Then, the dimensional parameters R_i in Eqs. (1)–(12) should be replaced by their counterparts r_i. In the subsequent subsections, we will study the manipulator with r_i.

4.2.1 Workspace Performance. For the manipulator studied here, *Deduction 1* indicates that only the workspace along the y axis can be considered in the design process. In this paper, workspace is a generalized terminology. *Positional workspace* (PW) is

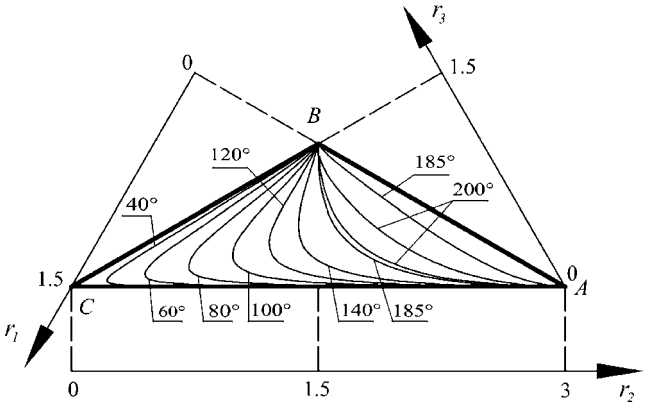

Fig. 4 Atlas of the minimum MRC

the position region about the Cartesian coordinate and, *orientational workspace* (OW) is the orientation region about the rotational DOF of the manipulator.

DEFINITION 1. *The usable workspace is defined as the workspace that the manipulator can reach continuously with a specified assembly mode*.

As is well known, if a manipulator changes its assembly mode, it must pass a singular pose. Therefore, according to the definition, a usable workspace is the workspace without the singularity inside but bounded by singular locus.

DEFINITION 2. *The usable positional workspace (UPW) along the y axis, denoted as* $W_{y\text{–UP}}$, *is defined as the usable workspace that the manipulator can reach continuously with at least one orientation*.

The UPW is actually restricted by the first kind of singularity of the manipulator and can be obtained from Eqs. (1)–(3). From Eqs. (1) and (2), because $R_2^2-(R_3-R_1+y)^2$ should be greater than or equal to (GE) 0, one obtains

$$-(r_1+r_2-r_3) \leqslant y \leqslant r_1+r_2-r_3 \tag{18}$$

Similarly, from Eq. (3), one writes

$$-\sqrt{r_2^2-(r_3-r_1\cos\phi)^2} \leqslant y \leqslant \sqrt{r_2^2-(r_3-r_1\cos\phi)^2} \tag{19}$$

in which y reaches its extremum when $\phi=0$. For the manipulator, because $\sqrt{r_2^2-(r_3-r_1)^2} \geqslant r_1+r_2-r_3$, $W_{y\text{–UP}}$ can be written as

$$W_{y\text{–UP}}=[y|-(r_1+r_2-r_3) \leqslant y \leqslant r_1+r_2-r_3] \tag{20}$$

Then, the area of $W_{y\text{–UP}}$ is $2(r_1+r_2-r_3)$ or $2(3-2r_3)$.

The above analysis shows that the motion range defined by Eq. (18) is included in that defined by Eq. (19). Equation (18) actually defines the boundaries of the UPW.

DEFINITION 3. *The constant-position usable workspace (CPUW), denoted as* $W_{\phi\text{–}y}$, *is defined as the orientations that the manipulator can reach continuously at a specified position* (y).

It is obvious that the CPUW will be different at different points. The CPUW can be evaluated by the MRC $\xi_{\max}$. For example, if $W_{\phi\text{–}y}=[\phi|-82° \leqslant \phi \leqslant 31°]$, the corresponding MRC is $\xi_{\max}=31°-(-82°)=113°$.

According to *Deduction* 2, in the design process of the manipulator, in order to make sure that the moving platform can reach the desired rotational capability, the MRC at the end point of the UPW is worthy of being investigated. In Eq. (12), the MRC $\xi_{\max}$ at $y=r_1+r_2-r_3$, which is referred to as the minimum MRC, is related to the three parameters r_i $(i=1,2,3)$. The relationship between the minimum MRC and the three parameters is shown in Fig. 4, where the value denotes the MRC at the end point of the UPW. To plot the atlas of Fig. 4, one should first calculate every $\xi_{\max}$ value at $y=r_1+r_2-r_3$ for each non-dimensional manipulator with r_1, r_2, and r_3, which is included in the design space. Using Eq. (17), one can then obtain the relationship between the minimum MRC and the two orthogonal coordinates s and t. This relationship is practically used to plot the atlas in the system with s and t. The subsequent atlas is also plotted using the same method. Figure 4 shows not only the relationship between $\xi_{\max}$ and the two orthogonal coordinates but that between $\xi_{\max}$ and the three nondimensional parameters as well. What we really are most concerned about is the later relationship, for which s and t are not shown in the figure. From this atlas, we can see that a longer r_2 usually leads to a better rotational capability.

The distribution of the minimum MRC in the design space indicates that if the r_3 value is near to 1.5 the index will be very poor. A smaller r_2 or larger r_1 usually results in lower rotational capability for the manipulator. And a manipulator with larger r_2 and smaller r_1 can have higher rotational capability.

4.2.2 Conditioning Index (CI). The Jacobian matrix is heavily dependent on the geometric parameters of the manipulator. Therefore, there is a subtle relationship between the performance and link lengths. For such reasons, almost all of the proposed indices are based on the Jacobian matrix. The conditioning index (CI) [14,27] is one of such indices.

Mathematically, the condition number of a matrix can be used in numerical analysis to estimate the error generated in the solution of a linear system of equations by the error on the data. When applied to the Jacobian matrix, the condition number will give a measure of the accuracy of the control of the manipulator. The *local conditioning index* (LCI) is defined as the reciprocal of the condition number of Jacobian matrix. That is

$$\mu=1/\kappa, \quad 0 \leqslant \mu \leqslant 1 \tag{21}$$

where κ is the condition number of the Jacobian matrix, and $\kappa=\|\mathbf{J}^{-1}\|\|\mathbf{J}\|$, in which $\|\cdot\|$ denotes the Euclidean norm of a matrix. The LCI is actually the distance between a specified pose and the singularity. It can be used to evaluate the dexterity, isotropy, as well as the static stiffness of a parallel manipulator [28–30]. This number is to be kept as large as possible.

Notice that elements in matrix $\mathbf{J}$ have no identical dimensions. To deal with the nonhomogeneity of the matrix, all elements in the third column should be divided by a link parameter. In this manipulator, there are three link parameters, i.e., $R_1(r_1)$, $R_2(r_2)$ and $R_3(r_3)$. From Sec. 2.4, we know that $R_1(r_1)=0$ will lead the manipulator to the singularity. Therefore, the selected link parameter cannot be $R_1(r_1)$. Any one of the left two parameters can be the candidate. The selection will not affect the distribution of the global conditioning index (GCI) in the design space but the GCI in magnitude. In this paper, in the process of calculating μ, the elements are divided by $R_3(r_3)$.

As we know, the LCI will be different at different pose. The GCI [27,31] can evaluate the global performance in the workspace of the parallel manipulator. The GCI is defined in a general form

$$\eta=\int_W \mu dW \Big/ \int_W dW \tag{22}$$

in which W denotes the workspace of the parallel manipulator.

In the case of the manipulator studied herein, the LCI μ is the function of y and ϕ. The GCI can be rewritten as

$$\eta=\int_{W_{\phi\text{–}y}}\int_{W_{y\text{–UP}}} \mu(y,\phi)dyd\phi \Big/ \int_{W_{\phi\text{–}y}}\int_{W_{y\text{–UP}}} dyd\phi \tag{23}$$

which is actually the average of the LCI μ with respect to the UPW and orientational workspace of the manipulator. The average is calculated by adding up the μ in every point in the workspaces and then dividing it with the number of points considered in the workspaces. This index should be kept as large as possible.

Figure 5 illustrates the relationship between the GCI η and the three parameters r_i $(i=1,2,3)$. The value in the atlas denotes the

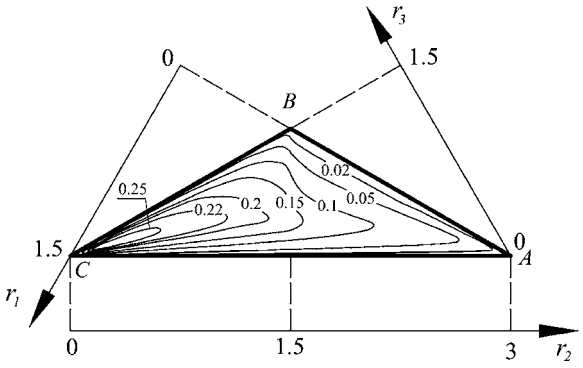

Fig. 5 Atlas of the GCI η

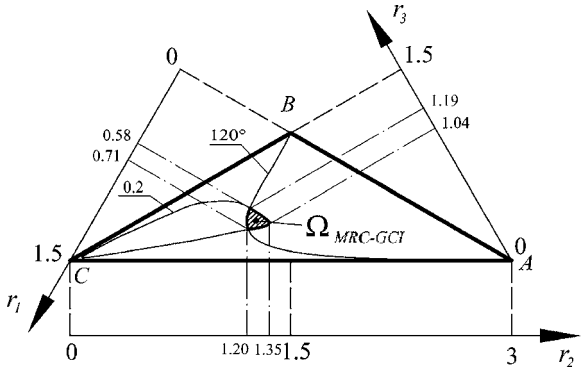

Fig. 6 The optimal region considering the MRC and GCI criteria

corresponding GCI of a manipulator with r_i. The atlas indicates that the index of a manipulator within the region $\Omega_1 = [(r_1, r_2, r_3) | 0.58 < r_1 < 1.44, 0.09 < r_2 < 1.35, r_3 = 3 - r_1 - r_2]$ is better. The GCI is usually proportional to the parameter r_1. That is to say that if r_1 is near to 0.0, the GCI is very poor. This is identical with the result of the singularity analysis. If the parameter r_3 is near to 1.5, the index is also very poor. This is obvious. The manipulator with $r_3 = 1.5$ is actually in the singularity.

4.3 Determination of the Link Lengths. The objective of this section is to determine the optimal parameters R_1, R_2, and R_3. This process consists of four steps: (a) using atlases to identify an optimum region in the design space taking into account the kinematic performance constraints; (b) selecting an optimum non-dimensional manipulator from the obtained region; (c) using LCI to determine a good-conditioning workspace (GCW); (d) comparing the GCW with the desired workspace to determine the parameters R_1, R_2, and R_3.

4.3.1 Optimum Region in the Design Space. In the previous subsection, the atlases of the MRC and GCI were obtained as shown in Figs. 4 and 5, respectively. From these atlases, we can easily understand the relationships between the indices and parameters r_i. This helps us to reach the design result. But, first, we need to generalize an optimal region taking into account the indices and atlases, which will decrease our object candidates.

Considering our objective, i.e., the ±50 deg tilting capability of the moving platform, the MRC ξ_{max} should be GE 100 deg. Please note that according to the definition of MRC and Fig. 2, the CPUW is delimited by singular configurations, where the manipulator will be out of control. If $\xi_{max} = 100$ deg is specified as the criterion for selecting a manipulator from Fig. 4, the manipulator will fail to reach the ±50 deg tilting capability. For such a reason, here, we define $\xi_{max} = 120$ deg as the lowest limit of the MRC. The optimal region of MRC is defined as $\Omega_{MRC} = [(r_1, r_2, r_3) | \xi_{max}(r_1, r_2, r_3) \geq 120 \text{ deg}]$.

The process of plotting the atlas of GCI shows that the GCI of a non-dimensional manipulator cannot exceed 0.3. To let the GCI be as large as possible, the optimal region of GCI can be defined as $\Omega_{GCI} = [(r_1, r_2, r_3) | \eta(r_1, r_2, r_3) \geq 0.20]$.

From Figs. 4 and 5, we can obtain an optimal region $\Omega_{MRC\text{-}GCI}$ considering the MRC and GCI criteria, i.e.,

$$\Omega_{MRC-GCI} = \Omega_{MRC} \cap \Omega_{GCI} \tag{24}$$

which is the shade region in Fig. 6.

4.3.2 Selection of a Candidate From the Optimum Region. From the optimal region $\Omega_{MRC\text{-}GCI}$, one can select a non-dimensional manipulator with r_1, r_2 and r_3, e.g., $r_1 = 0.60$, $r_2 = 1.34$, and $r_3 = 1.06$. Its UPW is $W_{y-UP} = [y | -0.88 \leq y \leq 0.88]$ and CPUW at $y = 0.88(-0.88) W_{\phi-y} = [\phi | -85.27 \text{ deg} \leq \phi \leq 48.84 \text{ deg}]$. The values of MRC at $y = 0.88(-0.88)$ and the GCI of the manipulator are $\xi_{max} = 134.11$ deg and $\eta = 0.2314$, respectively.

It is worth noting that the selected manipulator is not the most optimal result. It is one of the manipulators in the optimal region $\Omega_{MRC\text{-}GCI}$. Since the design issue is not a simple problem and, especially, MRC and GCI are not the only factors determining the design result, the designer can choose from among the candidates in this optimal region befittingly. It is fundamentally the designer's decision to choose which manipulator to use and this decision depends on the specified condition that the designer faces. In this paper, we select the manipulator with $r_1 = 0.60$, $r_2 = 1.34$ and $r_3 = 1.06$ merely as an example to present the proposed design method.

Figure 7 shows the distribution of LCI of the selected manipulator on its workspace.

4.3.3 Good-Conditioning Workspace of the Candidate. Figure 7 shows that some positions and orientations in the workspace are in or near the singularity. At those poses, the manipulator will be out of control, and thus, such poses should be excluded from the workspace.

DEFINITION 4. *The good-conditioning workspace (GCW) is defined as a usable workspace that the manipulator can reach with at least one good-conditioning pose. It contains two aspects: good-conditioning positional workspace (GCPW) and good-conditioning orientational workspace (GCOW). The GCPW is then defined as the UPW that the manipulator can reach with at least one good-conditioning orientation, while the GCOW is defined as the CPUW that the manipulator can have with the good-conditioning orientations*.

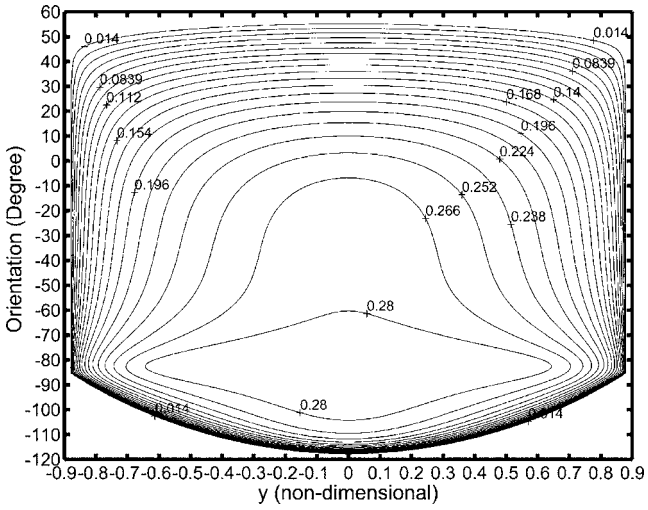

Fig. 7 Distribution of LCI on the workspace

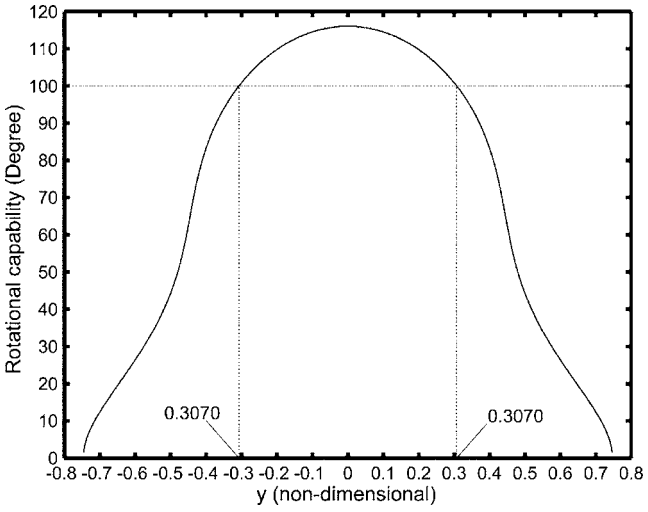

Fig. 8 Rotational capability on the GCPW

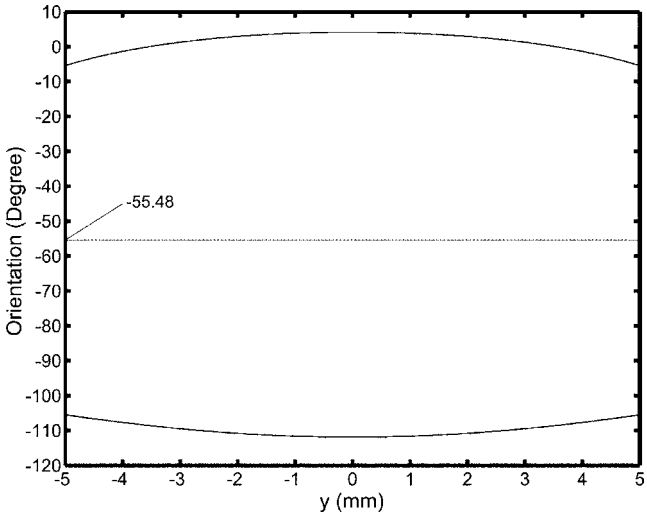

Fig. 9 GCOW on the GCPW of the dimensional manipulator

Remark. In the definition, a good-conditioning pose means the pose where the LCI of the manipulator is GE a specified LCI. The specified LCI is supposed to be a good-conditioning index. When the LCI at one pose is GE the specified LCI, we can say that the manipulator is in good condition.

For example, if the specified LCI is supposedly 0.25, the GCPW along the y axis of the manipulator with $r_1=0.60$, $r_2=1.34$ and $r_3=1.06$ will be $-0.7460 \leqslant y \leqslant 0.7460$, which can be obtained using the numerical method by letting $\mu=0.25$. The rotational capability of the manipulator along the y axis can be represented in Fig. 8, which shows that the rotational capability is best when $y=0$ and worst at the two end points of the GCPW.

Figure 8 shows that the rotational capability at $y=\pm 0.7460$ and their neighborhoods cannot satisfy the specification (±50 deg) on the tilting capability of the manipulator. Numerical calculation result shows that on the GCPW $-0.3070 \leqslant y \leqslant 0.3070$, the rotational capability at every point is GE 100 deg (see Fig. 8). Therefore, the length of the GCPW along the y axis, where the rotational capability at every point is GE 100 deg, is 0.6140(0.3070 $-(-0.3070)$). This is the final GCW that we ultimately aim for with respect to our specification.

4.3.4 Determination of the Dimensional Link Lengths. In the previous subsections, a non-dimensional manipulator with link lengths $r_1=0.60$, $r_2=1.34$ and $r_3=1.06$ is selected from the optimum region. And the GCW along the y axis was obtained as $-0.3070 \leqslant y \leqslant 0.3070$ with a length of 0.6140. In this section, we will determine the dimensional link lengths of the manipulator with respect to the desired workspace, i.e., $y \times z = 10$ mm $\times 10$ mm.

PROPOSITION 4. *Quantitatively, the usable positional workspace (UPW) along the y axis of a dimensional manipulator with parameters $R_i=Dr_i$ is D time that of a non-dimensional manipulator with parameters r_i. The orientational workspaces of the two types of manipulators are the same as that of the other*.

Proof. The UPW of a non-dimensional manipulator is given by Eq. (20). Using Eq. (14) and substituting $R_i=Dr_i$ into Eq. (20) leads to $W_{y\text{-UP}}=[y|-(R_1+R_2-R_3)/D \leqslant y \leqslant (R_1+R_2-R_3)/D]$, which indicates that the UPW along the y axis of a manipulator with R_i is D time that of a manipulator with r_i. From Eq. (12), one can notice that the replacement of R_i by r_i does not change the value of $\xi_{\max}$.

PROPOSITION 5. *The GCPW of a dimensional manipulator with $R_i=Dr_i$ is also D time that of a non-dimensional manipulator with r_i. The GCOWs are the same as that of the other*.

Proof. The observation of the Eq. (11) shows that the Jacobian matrix with r_i and y is the same as that with $R_i=Dr_i$ and Dy. This leads to the same LCI values. The GCW is defined with respect to a specified LCI. Therefore, the GCWs have the relationships in PROPOSITION 5.

Therefore, according to the PROPOSITION 5, the scaling parameter D is actually the ratio of the desired workspace along the y axis to the GCPW along the y axis of the non-dimensional manipulator. Thus, for the design example, there is $D=10/0.6140=16.29$ mm. Using Eq. (14), the dimensional link lengths of the manipulator can be obtained as $R_1=9.77$ mm, $R_2=21.82$ mm, and $R_3=17.26$ mm.

PROPOSITION 6. *The GCI values of the manipulators with $R_i=Dr_i$ and r_i, respectively, are the same as those of the other*.

Proof. As mentioned above, the LCI at y for the manipulator with r_i is the same as that at Dy for the manipulator with $R_i=Dr_i$. The GCI is the average of LCI with respect to a workspace. If their workspaces have the D-time relationship, the GCI values with respect to their workspaces will be the same as the other.

DEFINITION 5. *The manipulators that have the characteristics of propositions 4, 5, and 6 are defined as the similarity manipulators. That means, for these manipulators, the positional workspaces are different in area, but identical in shape and the orientational workspaces and GCI values are the same as that of the other*.

Thus, all manipulators with parameters $R_i=Dr_i$ are *similarity manipulators*. If the manipulator with parameter r_i is defined as the *basic similarity manipulator*, the most important contribution of the developed design space is that all possible *basic similarity manipulators* can be included in this design space. This, in turn, guarantees global optimization. Accordingly, as it is possible to always obtain an optimum region by using the performance atlases, the design methodology proposed in this paper helps determine a set of possible solutions, and ideally, all the design solutions.

Deduction 3. If a *basic similarity manipulator* is optimal, all of its *similarity manipulators* will be optimum design results.

According to this deduction, because the non-dimensional parallel manipulator with $r_1=0.60$, $r_2=1.34$ and $r_3=1.06$ is from the optimum region $\Omega_{\text{MRC-GCI}}$, the dimensional manipulator $R_1=9.77$ mm, $R_2=21.82$ mm, and $R_3=17.26$ mm, which is one of the *similarity manipulators* and which satisfies the desired specification on positional workspace and rotational capability, is the optimized design.

The GCOW on the GCPW of the dimensional manipulator is shown in Fig. 9, where the upper and lower curves indicate the limits of the GCOW. For example, the GCOW at $y=\pm 5.0$ mm is $-105.48° \leqslant \phi \leqslant -5.48°$. Our objective is the ±50 deg tilting capa-

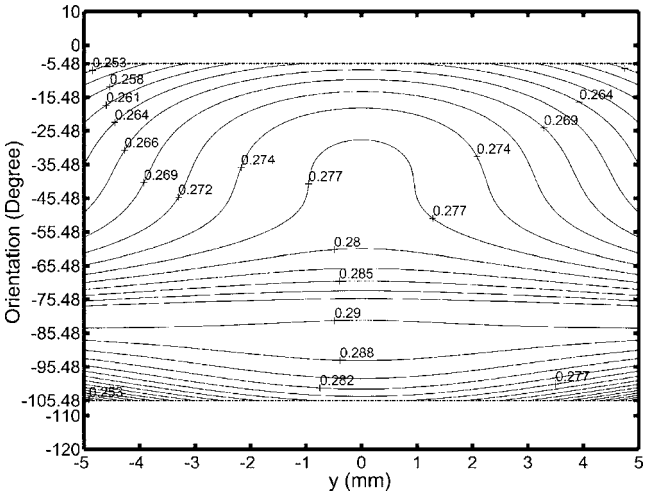

Fig. 10 Distribution of LCI at every section of the desired workspace of the dimensional parallel manipulator

bility at every point in the workspace. Thus, we need to specify the original orientation of the moving platform. At $y=\pm 5.0$ mm, there is $(-105.48^\circ$ to $-5.48^\circ)/2=-55.48^\circ$, which is the middle orientation between -105.48 deg and -5.48 deg of the moving platform at the point. From Fig. 9, we can see that the distance from the lower and upper GCOW limit curves to the line $\phi=-55.48^\circ$ is GE 50. Then, the original orientation can be given with respect to the GCOW when $y=\pm 5.0$ mm. If the original orientation is defined as ϕ_O, there is $\phi_O=-55.48$ deg, from which the moving platform can tilt ± 50 deg angle at every point in the GCPW.

Considering the desired workspace along both the y and z axes and the expected tilting capability, inputs for the three actuators can be $z_1, z_2=[17.89, 31.68]$ mm and $z_3=[-1.91, 29.55]$ mm, respectively, which can be calculated from the inverse kinematic Eqs. (1)–(3).

All in all, to satisfy the specification such as the positional workspace $y\times z=10$ mm $\times 10$ mm and the ± 50 deg tilting capability at every point within this workspace, the parameters of an optimized manipulator with respect to workspace, rotational capability and GCI can be $R_1=9.77$ mm, $R_2=21.82$ mm, $R_3=17.26$ mm, $z_1, z_2=[17.89, 31.68]$ mm, and $z_3=[-1.91, 29.55]$ mm. The original orientation ϕ_O should be -55.48 deg. The LCI on every workspace section along the z axis is shown in Fig. 10, which shows that the LCI is GE 0.25 within the workspace.

4.4 Flow Chart of the Methodology. The flowchart of the methodology determining the link lengths of the 3-DOF parallel manipulator is shown in Fig. 11.

One can see that in the developed design methodology the developed design space and atlases are primarily important. This idea was also introduced in [30–32], where the design space was referred to as *the physical model of the solution space* (PMSS). But, these papers only concentrated on the manipulators with revolute actuators, and, in fact, in these papers the PMSS was only used to analyze the performance of the manipulators. They did not show how a final optimal can be reached. Therefore, in this paper, the design issue is presented systematically based on the idea, and the process to optimize the non-dimensional and dimensional parameters of a 3-DOF parallel manipulator with linear actuators is illustrated in detail. This newly proposed methodology is considered to be acceptable and be used in practice by others.

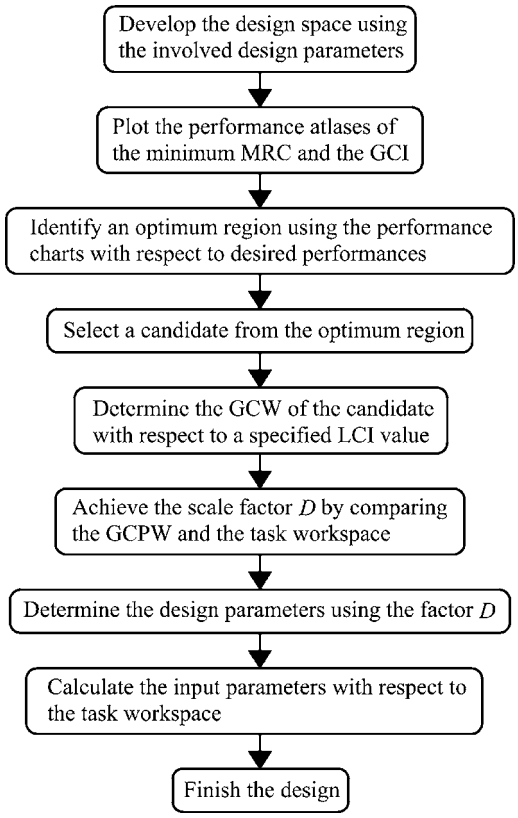

Fig. 11 The flow chart of determination of the link lengths for the 3-DOF parallel manipulator

5 Conclusions

This paper proposes a new optimal design method to determine the geometric parameters of a 3-DOF parallel manipulator where no angle parameter is involved in the design. The key issue of this design method is to establish a geometric design space based on the involved geometric parameters, which can embody all *basic similarity manipulators*. Then, atlases of desired indices can be plotted. These atlases can be used to identify an optimal region, from which an ideal candidate can be selected. The real-dimensional parameters can be reached by considering the desired workspace and the *good-conditioning workspace* of the non-dimensional manipulator. Compared with other design methods, the proposed methodology has some advantages as follows: (a) one performance criterion corresponds to one atlas, which can visually and globally show the relationship between the criterion and design parameters; (b) for such a reason in (a), the fact that some performance criteria are antagonistic is no longer a problem in the design; (c) the optimum design process can consider multi-objective functions or multicriteria, and also guarantees the optimal result; and, finally, (d) as the optimum design can be carried out by using atlases; this methodology shall be said to be acceptable in practice.

Acknowledgment

This work was supported by the NRL Program on Next Generation Parallel Mechanism Platforms, the Brain Korea 21 Program in Mechanical and Aerospace Engineering at SNU, and partly by the National Natural Science Foundation of China (Grant No. 50505023.

References

[1] Liu, X.-J., Wang, J., Gao, F., and Wang, L.-P., 2001, "On the Analysis of a New Spatial Three Degrees of Freedom Parallel Manipulator," IEEE Trans.

Rob. Autom., **17**(6), pp. 959–968.
[2] Kong, X., and Gosselin, C. M., 2002, "Type Synthesis of 3-DOF Spherical Parallel Manipulators Based on Screw Theory," *Proceedings of DETC'02 ASME 2002 Design Engineering Technical Conferences and Computer and Information in Engineering Conference*, Montreal, Canada, DETC2002/MECH-34259, Sponsor American Society of Mechanical Engineering.
[3] Di Gregorio, R., 2002, "A New Family of Spherical Parallel Manipulators," Robotica, **20**(4), pp. 353–358.
[4] Hess-Coelho, Tarcisio A., 2006, "Topological Synthesis of a Parallel Wrist Mechanism," ASME J. Mech. Des., Paper No. MD-04–1195.
[5] Kim, H. S., and Tsai, L.-W., 2003, "Design Optimization of a Cartesian Parallel Manipulator," ASME J. Mech. Des., **125**(1), pp. 43–51.
[6] Chablat, D., and Wenger, P., 2003, "Architecture Optimization of a 3-DOF Translational Parallel Mechanism for Machining Applications, the Orthoglide," IEEE Trans. Rob. Autom., **19**(3), pp. 403–410.
[7] Liu, X.-J., Jeong, J., and Kim, J., 2003, "A Three Translational DOFs Parallel Cube-Manipulator," Robotica, **21**(6), pp. 645–653.
[8] Carricato, M., and Parenti-Castelli, V., 2003, "Kinematics of a Family of Translational Parallel Mechanisms With Three 4-DOF Legs and Rotary Actuators," J. Rob. Syst., **20**(7), pp. 373–389.
[9] Jin, Q., and Yang, T.-L., 2004, "Theory for Topology Synthesis of Parallel Manipulators and Its Application to Three-Dimension-Translation Parallel Manipulators," ASME J. Mech. Des., **126**, pp. 625–639.
[10] Liu, X.-J., and Wang, J., 2003, "Some New Parallel Mechanisms Containing the Planar Four-Bar Parallelogram," Int. J. Robot. Res., **22**(9), pp. 717–732.
[11] Ottaviano, E., and Ceccarelli, M., 2002, "Optimal Design of CaPaMan (Cassino Parallel Manipulator) With a Specified Orientation Workspace," Robotica, **20**, pp. 159–166.
[12] Kosinska, A., Galicki, M., and Kedzior, K., 2002, "Determination of Parameters of 3-DOF Spatial Orientation Manipulators for a Specified Workspace," Robotica, **20**, pp. 179–183.
[13] Ceccarelli, M., and Ottaviano, E., 2002, "A Workspace Evaluation of an Eclipse Robot," Robotica, **20**, pp. 299–313.
[14] Gosselin, C. M., and Angeles, J., 1989, "The Optimum Kinematic Design of a Spherical Three Degree-of-Freedom Parallel Manipulator," ASME J. Mech., Transm., Autom. Des., **111**, pp. 202–207.
[15] Merlet, J.-P., 1997, "Designing a Parallel Manipulator for a Specific Workspace," Int. J. Robot. Res., **16**, pp. 545–556.
[16] Arsenault, M., and Boudreau, R., 2006, "Synthesis of Planar Parallel Mechanisms While Considering Workspace, Dexterity, Stiffness and Singularity Avoidance," ASME J. Mech. Des., Paper No. MD-04–1250 (in press).
[17] Schonherr, J., 2000, "Evaluation and Optimum Design of Parallel Manipulators Having a Defined Workspace," *Proceedings of the ASME Design Engineering Technical Conference and Computers and Information in Engineering Conference*, Baltimore, DETC2000/MECH-14092, Sponsor American Society of Mechanical Engineerings.
[18] Stoughton, R. S., and Arai, T., 1993, "A Modified Stewart Platform Manipulator With Improved Dexterity," IEEE Trans. Rob. Autom., **9**(2), pp. 166–173.
[19] Carretero, J. A., Podhorodeski, R. P., Nahon, M. A., and Gosselin, C. M., 2000, "Kinematic Analysis and Optimization of a New Three Degree-of-Freedom Spatial Parallel Manipulator," ASME J. Mech. Des., **122**, pp. 17–24.
[20] Ryu, J., and Cha, J., 2001, "Optimal Architecture Design of Parallel Manipulators for Best Accuracy," *Proceedings of the 2001 IEEE/RSJ International Conference on Intelligent Robots and Systems*, Maui, Hawwaii, USA, pp. 1281–1286.
[21] Zhang, D., Wang, L., and Lang, S. Y. T., 2005, "Parallel Kinematic Machines: Design, Analysis and Simulation in an Integrated Virtual Environment," ASME J. Mech. Des., **127**, pp. 580–588.
[22] Fattah, A., and Agrawal, S. K., 2005, "On the Design of Cable-Suspended Planar Parallel Robots," ASME J. Mech. Des., Paper No. MD-04–1111 (in press).
[23] Stock, M., and Miller, K., 2003, "Optimal Kinematic Design of Spatial Parallel Manipulators: Application to Linear Delta Robot," ASME J. Mech. Des., **125**(2), pp. 292–301.
[24] Merlet, J.-P., 2002, "Still a Long Way to Go on the Road for Parallel Mechanisms," A keynote speech presented in *ASME 27th Biennial Mechanisms and Robotics Conf.*, Montréal, Canada, Sept. 29–Oct. 2.
[25] Boudreau, R., and Gosselin, C. M., 1999, "The Synthesis of Planar Parallel Manipulators With a Genetic Algorithm," ASME J. Mech. Des., **121**, pp. 533–537.
[26] Merlet, J.-P., 2001, "An Improved Design Algorithm Based on Interval Analysis for Parallel Manipulator With Specified Workspace," *Proceedings of IEEE International Conference on Robotics and Automation*, Seoul, Korea, pp. 1289–1294.
[27] Gosselin, C., and Angeles, J., 1991, "A Global Performance Index for the Kinematic Optimization of Robotic Manipulators," ASME J. Mech. Des., **113**, pp. 220–226.
[28] Angeles, J., and López-Cajún, C., 1992, "Kinematic Isotropy and the Conditioning Index of Serial Robotic Manipulators," Int. J. Robot. Res., **11**(6), pp. 560–571.
[29] Salisbury, J. K., and Craig, J. J., 1982, "Articulated Hands: Force Control and Kinematic Issues," Int. J. Robot. Res., **1**(1), pp. 4–12.
[30] Liu, X.-J., Wang, J., Gao, F., and Wang, L.-P., 2002, "The Mechanism Design of a Simplified 6-DOF 6-RUS Parallel Manipulator," Robotica, **20**, pp. 81–91.
[31] Gao, F., Liu, X.-J., and Gruver, W. A., 1998, "Performance Evaluation of Two-Degree-of-Freedom Planar Parallel Robots," Mech. Mach. Theory, **33**, pp. 661–668.
[32] Liu, X.-J., Wang, J., and Zheng, H., 2003, "Workspace Atlases for the Computer-Aided Design of the Delta Robot," Proc. Inst. Mech. Eng., Part C, Prog. Low Temp. Phys., **217**, pp. 861–869.